OXFORD

The ABCD study: brain heterogeneity in intelligence during a neurodevelopmental transition stage

Qi Zhao [iD] [1,†], Valerie Voon [2,†], Lingli Zhang [3], Chun Shen [4], Jie Zhang [4,*], Jianfeng Feng [4,5,*]

[1]School of Mathematical Sciences, Fudan University, Shanghai 200433, PR China,
[2]Department of Psychiatry, University of Cambridge, Cambridge CB2 0SZ, UK,
[3]Developmental and Behavioral Pediatric & Child Primary Care Department, Ministry of Education-Shanghai Key Laboratory of Children's Environmental Health, Xinhua Hospital, Shanghai Jiao Tong University School of Medicine, Shanghai 200092, PR China,
[4]Institute of Science and Technology for Brain Inspired Intelligence, Fudan University, Shanghai 200433, PR China,
[5]Department of Computer Science, University of Warwick, Coventry CV4 7AL, UK

*Corresponding authors: Professor Jianfeng Feng, Institute of Science and Technology for Brain Inspired Intelligence, Fudan University, Shanghai 200433, PR China.
Email: jianfeng64@gmail.com; Professor Jie Zhang, Institute of Science and Technology for Brain Inspired Intelligence, Fudan University, Shanghai 200433, PR China. Email: zhangjie80@fudan.edu.cn.
[†]Qi Zhao and Valerie Voon have contributed equally to this work

A complex curvilinear relationship exists between intelligence and age during the neurodevelopment of cortical thickness. To parse out a more fine-grained relationship between intelligence and cortical thickness and surface area, we used a large-scale data set focusing on a critical transition juncture in neurodevelopment in preadolescence. Cortical thickness was derived from T1-weighted structural magnetic resonance images of a large sample of 9- and 11-year-old children from the Adolescent Brain Cognitive Development study. The NIH Toolbox Cognition Battery composite scores, which included fluid, crystallized, and total scores, were used to assess intelligence. Using a double generalized linear model, we assessed the independent association between the mean and dispersion of cortical thickness/surface area and intelligence. Higher intelligence in preadolescents was associated with higher mean cortical thickness in orbitofrontal and primary sensory cortices but with lower thickness in the dorsolateral and medial prefrontal cortex and particularly in the rostral anterior cingulate. The rostral anterior cingulate findings were particularly evident across all subscales of intelligence. Higher intelligence was also associated with greater interindividual similarity in the rostral cingulate. Intelligence during this key transition juncture in preadolescence appears to reflect a dissociation between the cortical development of basic cognitive processes and higher-order executive and motivational processes.

Key words: adolescence; cognitive process; cortical thickness; intelligence; surface area.

Introduction

Intelligence develops rapidly during adolescence, a period characterized by profound brain neurodevelopment and maturation, and critically anchors higher-order cognitive function (Emery and Clayton 2005; Gilbert et al. 2005; Arain et al. 2013; Fuhrmann et al. 2015). Markers of neural substrates in gray matter regions have shown a close relationship to intellectual ability (Posthuma et al. 2002; Genc et al. 2018). General intelligence shows a strong relationship to cortical thickness (Posthuma et al. 2002; Narr et al. 2007; Pietschnig et al. 2015) and appears to share similar genetic substrates (Brans et al. 2010). Thus, understanding the relationship between neural biomarkers and intelligence during key critical periods of neurodevelopment might highlight important biomarkers of resilience.

Age has a marked influence on the relationship between intelligence and cortical thickness, with age within childhood and adolescence demonstrating an effect in opposing directions (Sowell et al. 2004; Karama et al. 2011). In a large longitudinal study in children

(Shaw et al. 2006), early childhood (3.8–8.4 years old) showed a predominantly negative correlation between intelligence and cortical gray matter thickness which shifted in late childhood (8.6–11.7 years old) to a pronounced positive correlation. These correlations were found in specific prefrontal cortices, including the superior frontal gyrus, dorsal medial prefrontal cortex, and medial orbitofrontal cortices. This shift in the direction of correlation has been attributed to the dynamic nature of neurodevelopment, hence impacting the neuroanatomical expression of intelligence in children and adolescents. Here, we sought to investigate the relationship between intelligence and gray matter within a tight age distribution at what appears to be a critical transition juncture when the direction of correlation between cortical thickness and intelligence was shown to shift (Shaw et al. 2006), thus controlling for age and neurodevelopmental differences during a period in which the brain is developing rapidly (Ostby et al. 2009; Brown and Jernigan 2012).

Previous studies focusing on the correlation between brain morphology and intelligence quotient (IQ) have

focused on the association between the group means of neuroimaging measures and IQ rather than interindividual variability, or the dispersion within the group. However, genetic and environmental factors are increasingly recognized to play critical roles in contributing to individual variability in brain structure (Gu and Kanai 2014; Alnaes et al. 2019). Thus, we use the dispersion model in the double generalized linear model (DGLM) (Smyth and Verbyla 1999; Paula 2013) to quantify the individual structure differences related to such complex factors as environment and genes. We included structural magnetic resonance imaging (MRI) scans from >10 000 subjects from the Adolescent Brain Cognitive Development (ABCD) Study (Casey et al. 2018), focusing on a narrow age span (9–11 years old), and identified the independent relationships between IQ and cortical thickness/surface area from both mean and variability using DGLM, which allows the simultaneous modeling of mean and dispersion in a generalized linear model context (Smyth and Verbyla 1999). All codes are available at GitHub (https://github.com/q1zhao/dglmThicknessIQ).

Materials and methods
Participants
The data set used for this investigation was selected from the Annual Curated Data Release 2.0.1 from the ABCD consortium (https://abcdstudy.org/index.html) which contains >11 000 children aged 9–11 years, recruited from 21 centers throughout the United States of America, with a diverse range of geographic, socioeconomic, ethnic, and health backgrounds (Casey et al. 2018; Hagler et al. 2019). Our sample includes 10 652 subjects (ages: 9–11 years, 5097 females) scanned with three 3 Tesla (T) scanner platforms: Siemens Prisma, General Electric 750, and Phillips from 21 sites. From 11 076 subjects, 424 were removed following quality control (Hagler et al. 2019) using FreeSurfer v5.3.0, and we removed subjects who lacked cognitive scores. More details of the subjects and the collection and preprocessing parameters of the data are provided at the ABCD website (https://abcdstudy.org/scientists/protocols/) and are also are described elsewhere (Casey et al. 2018; Hagler et al. 2019).

Procedure and material
We obtained preprocessed structural imaging data (T1) using the ABCD pipeline, with all the data preprocessing procedures performed by the ABCD team as described in their image processing paper (Hagler et al. 2019). Sex, age, and mean thickness are reported in Table 1. Cortical thickness and surface area were analyzed using FreeSurfer 5.3.0 using the Destrieux atlas (Destrieux et al. 2010) from the ABCD preprocessing, which includes 148 regions. We also analyzed the correlation between different scores and covariates like age, gender, and site (Supplementary Fig. S1). The DGLM models were employed to separately model the relationship between brain cortical thickness/surface area and the three

IQ scores: general intelligence (g), fluid intelligence (gF), and crystallized intelligence (gC). Among them, g can be quantified as the weighted sum of gF and gC.

The ABCD Consortium used the NIH Toolbox Cognition Battery (NIHTB-CB) composite scores (Luciana et al. 2018), which has previously been validated as a means of measuring IQ (Heaton et al. 2014). gF refers to the ability to generate, transform, and manipulate different types of novel information in real time, which is correlated with a number of important skills (Deary and Caryl 1997; Unsworth et al. 2014; Zaval et al. 2015); while gC is sometimes described as verbal ability and is more dependent on accumulated experience. The NIHTB-CB included a total score composite (g), a crystalized intelligence composite (gC) (the Toolbox Picture Vocabulary Task and the Toolbox Oral Reading Recognition Task), and a fluid intelligence composite (gF) (the Toolbox Pattern Comparison Processing Speed Test, the Toolbox List Sorting Working Memory Test, the Toolbox Picture Sequence Memory Test, the Toolbox Flanker Task, and the Toolbox Dimensional Change Card Sort Task) (Akshoomoff et al. 2013). These composite scores show good test–retest reliability in both children and adults as well as validity in children (Akshoomoff et al. 2013; Heaton et al. 2014) and are highly correlated ($r = 0.89$) with IQ scores measured with the WAIS-IV (Heaton et al. 2014). Although the age span was narrow, intelligence is significantly correlated with age. Therefore, we used age-corrected standard scores (detailed explanation is given in the Supplementary Materials) in our study.

Statistical analysis
Statistical analyses of demographic data and test scores were conducted using R (3.6.0; https://www.r-project.org/) and MATLAB (2019a, The MathWorks, Inc., Natick, Massachusetts, United States). Age, sex, and site were first regressed as nuisance variables using a generalized additive model (GAM) (Diederich 2007). Then, DGLM (Efron 1986; Smyth 1989) was proposed to model the relationship between cortical thickness/surface area and intelligence. The generalized linear models assume that the dispersion parameter is fixed. However, especially in analyzes of experiments and quality control, there may be a considerable influence of external factors on the variability of models. Thus, the assumption that the dispersion parameter is fixed becomes strong. The DGLM iteratively fits a generalized linear model of the mean parameter and a second generalized linear model of the variability parameter on the deviance of the first model. Cortical thickness statistic map (t statistics) were corrected for multiple comparisons using false discovery rate (FDR) correction (Benjamini and Hochberg 1995) (whole brain FDR-corrected P value < 0.05 was considered to be significant).

Table 1. Sample characteristics.

Characteristic	Aggregate ($n = 10\,652$), mean	Standard deviation
Age	118.97 (-month-old)	7.46
Gender		
Male	5555	
Female	5097	
Total intelligence	100.58	17.89
Crystallized intelligence	105.69	18.25
Picture vocabulary task	106.9428	16.9574
Oral reading recognition task	102.5695	19.0931
Fluid intelligence	95.75	17.28
Pattern Comparison Processing Speed Test	93.9251	21.9852
List Sorting Working Memory test	100.6641	14.7064
Picture Sequence Memory test	101.1097	16.1116
Flanker task	95.4679	13.5688
Dimensional Change Card Sort task	96.7827	15.1717
Cortical thickness (mm)	2.7756	0.1051
Surface area (whole brain, mm^2)	1.86e+05	1.81e+04

GAM, R-Package: mgcv (Wood 2017)

To control for the age, gender, and site effects, we ran GAMs on each ROI analysis using the following model:

$$Y_i \sim s\,(\text{age}) + \text{gender} + \text{Scanner}. \quad i = 1, 2, \ldots, M, \quad (1)$$

where Y_i represents the cortical thickness in each brain region, and s is a smooth function estimated from the data. M is the number of brain regions.

DGLM, R-Package: dglm (Dunn and Smyth 2012)

The DGLM was fitted using the following model for the mean and dispersion. Modeling the dispersion is important to obtain correct mean parameter estimates, particularly if dispersion varies as a function of the predictor and further allows for systematic investigation into factors associated with dispersion.

$$\text{Mean model}: \quad m_i = \mu + \text{Age}\beta_{\text{age}} + \text{Sex}\beta_{\text{sex}} + \text{IQ}\beta_{cs}$$
$$i = 1, 2, \ldots, M, \quad (2)$$
[[DmEquation2]]

$$\text{Dispersion model}: \quad \sigma_i = \upsilon + \text{Age}\gamma_{\text{age}} + \text{Sex}\gamma_{\text{sex}} + \text{IQ}\gamma_{cs}$$
$$i = 1, 2, \ldots, M. \quad (3)$$
[[DmEquation3]]

Here, we assume cortical thickness Y_i follows a normal distribution with expectation m_i and variance σ_i^2, and σ_i is also a function rather than a constant like m_i. All β, γ are the parameters to be estimated. For a more intuitive explanation of the model, Supplementary Figure S2 shows a general view of the relationship between different kinds of data distribution and DGLM.

On an exploratory basis, we also evaluated DGLM analyses correlating with the mean and dispersion of sub-scales contributing to the measures of gC and gF (Supplementary Materials).

Results
Associations between mean cortical thickness and intelligence

Mean cortical thickness showed a differential relationship in the direction of correlation, with g, gC, and gF demonstrating an anterior–posterior differential in the whole brain axis. Mean cortical thickness was predominantly negatively correlated with g (Fig. 1A), gC, and gF (Fig. 2) in dorsolateral and mesial frontal regions. The most prominent negative correlation was observed in the bilateral rostral anterior cingulate (Brodmann areas [BAs] 24 and 32) and also in the superior and middle frontal gyri (extending to premotor areas) and in inferior frontal gyri, the medial suborbital sulcus, and the dorsomedial prefrontal cortex extending to the supplementary motor area. By contrast, mean g, gC, and gF were positively correlated with orbitofrontal cortices and most posterior brain regions, particularly within the postcentral primary sensory cortices, temporo-occipital junction (BA 39), and mesial temporal and occipital cortices. Controlling for total brain thickness as a cofactor in the model did not influence the association between gF or gC and cortical thickness.

We further examined the relationship between the subscales contributing to gC and gF and cortical thickness. We show a negative correlation between the mean cortical thickness in the rostral anterior cingulate identified in the correlations of g, gC, and gF and scores across "all" subscales contributing to gC and gF (Supplementary Figs S3 and S4).

We also secondarily examined mean cortical surface area which was globally positively associated with g (Fig. 3A), gC (Supplementary Fig. S5A), and gF (Supplementary Fig. S6A). There were no negative correlations observed.

A) The mean model of cortical thickness and total intelligence
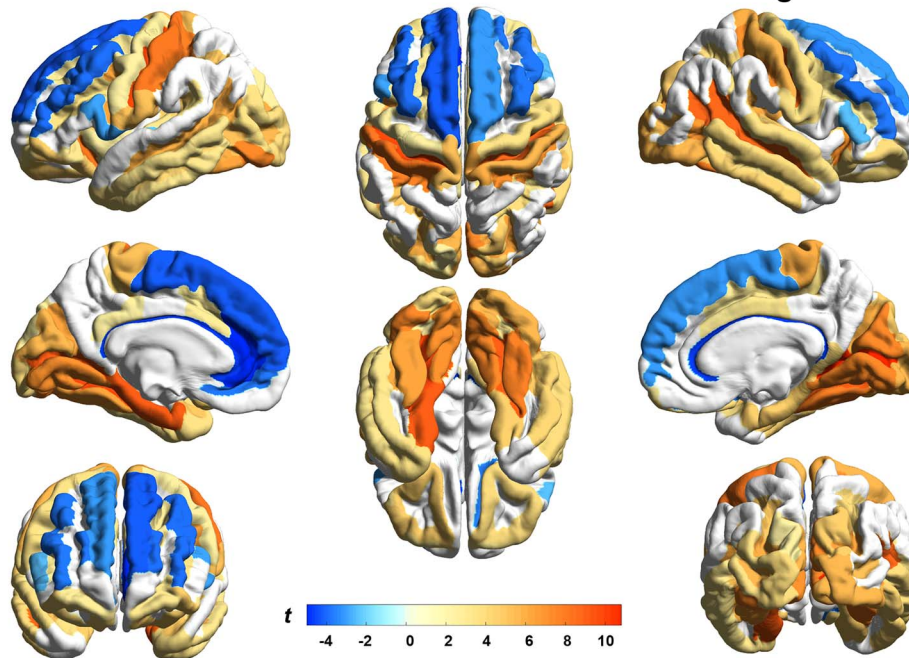
B) The dispersion model of cortical thickness and total intelligence
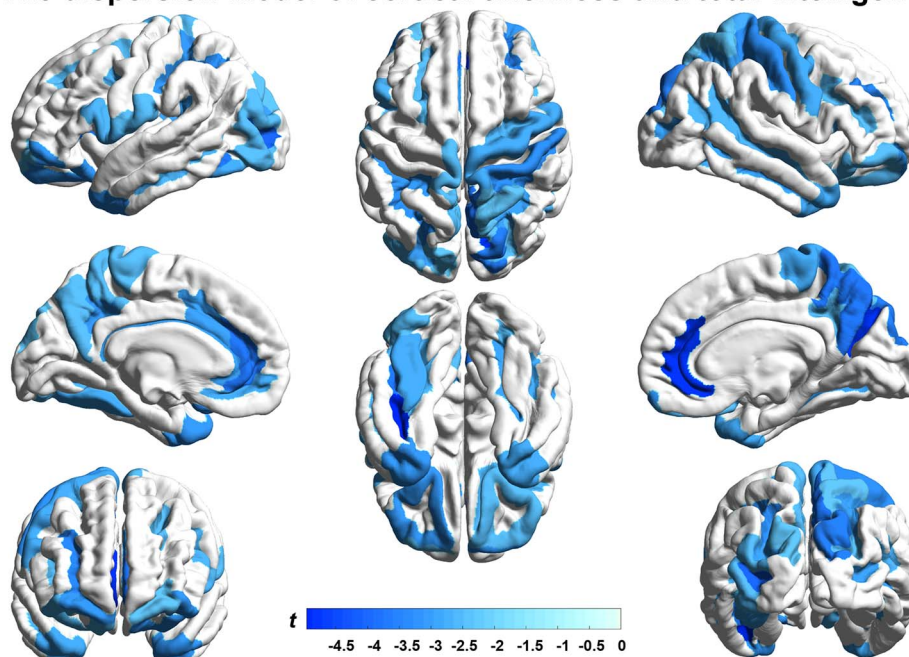
Fig. 1. Regions of interest showing cortical thickness and dispersion significantly associated with intelligence in (A) mean and (B) dispersion model. Cortical regions of interest for which *P* value < FDR-corrected (0.05) are shown based on the Destrieux atlas.

### Associations between interindividual dispersion of cortical thickness and intelligence

The DGLM also independently modeled the relationship between intelligence measures and cortical thickness dispersion. The *g* measure was negatively associated with cortical thickness dispersion (Fig. 1B), and *gC* and *gF* measures were as well (Fig. 4, Supplementary Figs S7B and S8B). Across *g*, *gC*, and *gF* (Table 2), a negative correlation was observed particularly in rostral cingulate (BA 32; bilateral but particularly on the right) and in the right precuneus (BA 7), meaning that higher IQ measures were associated with lower interindividual cortical thickness variability or dispersion. Other negative correlations between *g*, with dispersion observed in the orbitofrontal cortex and right somatosensory cortex, were driven by negative correlations between *gC* and the right orbitofrontal cortex and *gF* and the right somatosensory cortex, respectively.

Table 2. The cortical brain regions with *t* and *p* values which their cortical thickness dispersion is significantly correlated with three intelligence (intelligence, crystallized intelligence) in the dispersion model and fluid intelligence, multiple comparisons FDR-adjusted *P* value < 0.05).

	Cortical region	Abbr.	L/R	Intelligence			Crystallized intelligence			Fluid intelligence		
				t value	P value	p-FDR	t value	P value	p-FDR	t value	P value	p-FDR
1	Anterior transverse collateral sulcus	S_collat_transv_ant	L	−4.96	7.15E-07	6.42E-06	−4.10	4.12E-05	2.44E-04	−4.23	2.40E-05	1.50E-04
2	Parieto-occipital sulcus*	S_parieto_occipital	R	−4.83	1.39E-06	1.14E-05	−4.71	2.54E-06	1.97E-05	−3.49	4.92E-04	2.13E-03
3	Anterior part of the cingulate gyrus and sulcus**	G_and_S_cingul-Ant	R	−4.75	2.05E-06	1.62E-05	−4.49	7.18E-06	4.83E-05	−3.40	6.67E-04	2.85E-03
4	Middle occipital sulcus and lunatus sulcus*	S_oc_middle_and_Lunatus	L	−4.06	4.85E-05	2.82E-04	−3.93	8.54E-05	4.68E-04	−2.77	5.55E-03	1.70E-02
5	Superior segment of the circular sulcus of the insula*	S_circular_insula_sup	L	−3.85	1.18E-04	6.26E-04	−2.92	3.55E-03	1.19E-02	−3.72	2.04E-04	9.89E-04
6	Anterior part of the cingulate gyrus and sulcus	G_and_S_cingul-Ant	L	−3.72	2.00E-04	9.81E-04	−3.70	2.14E-04	1.03E-03	−2.47	1.37E-02	3.41E-02
7	Precuneus	G_precuneus	R	−3.64	2.71E-04	1.28E-03	−3.28	1.04E-03	4.16E-03	−2.71	6.68E-03	1.95E-02
8	Lateral occipito-temporal sulcus*	S_oc-temp_lat	L	−3.61	3.02E-04	1.39E-03	−2.65	8.06E-03	2.29E-02	−3.39	7.13E-04	2.99E-03
9	Superior occipital gyrus*	G_occipital_sup	R	−3.55	3.88E-04	1.74E-03	−2.62	8.88E-03	2.46E-02	−3.38	7.16E-04	2.99E-03
10	Middle frontal sulcus	S_front_middle	R	−3.38	7.30E-04	3.03E-03	−2.69	7.11E-03	2.05E-02	−2.90	3.77E-03	1.25E-02
11	Postcentral sulcus*	S_postcentral	R	−3.26	1.10E-03	4.38E-03	−2.62	8.92E-03	2.46E-02	−2.88	4.02E-03	1.33E-02
12	Intraparietal sulcus and transverse parietal sulci*	S_intrapariet_and_P_trans	L	−3.19	1.42E-03	5.49E-03	−2.55	1.08E-02	2.86E-02	−2.79	5.34E-03	1.65E-02

*The thickness of these brain regions was significantly positively correlated with intelligence (FDR adjusted *P* value < 0.05) in the mean model. **The thickness of these brain regions was significantly negatively correlated with intelligence (FDR adjusted *P* value <0.05) in the mean model.
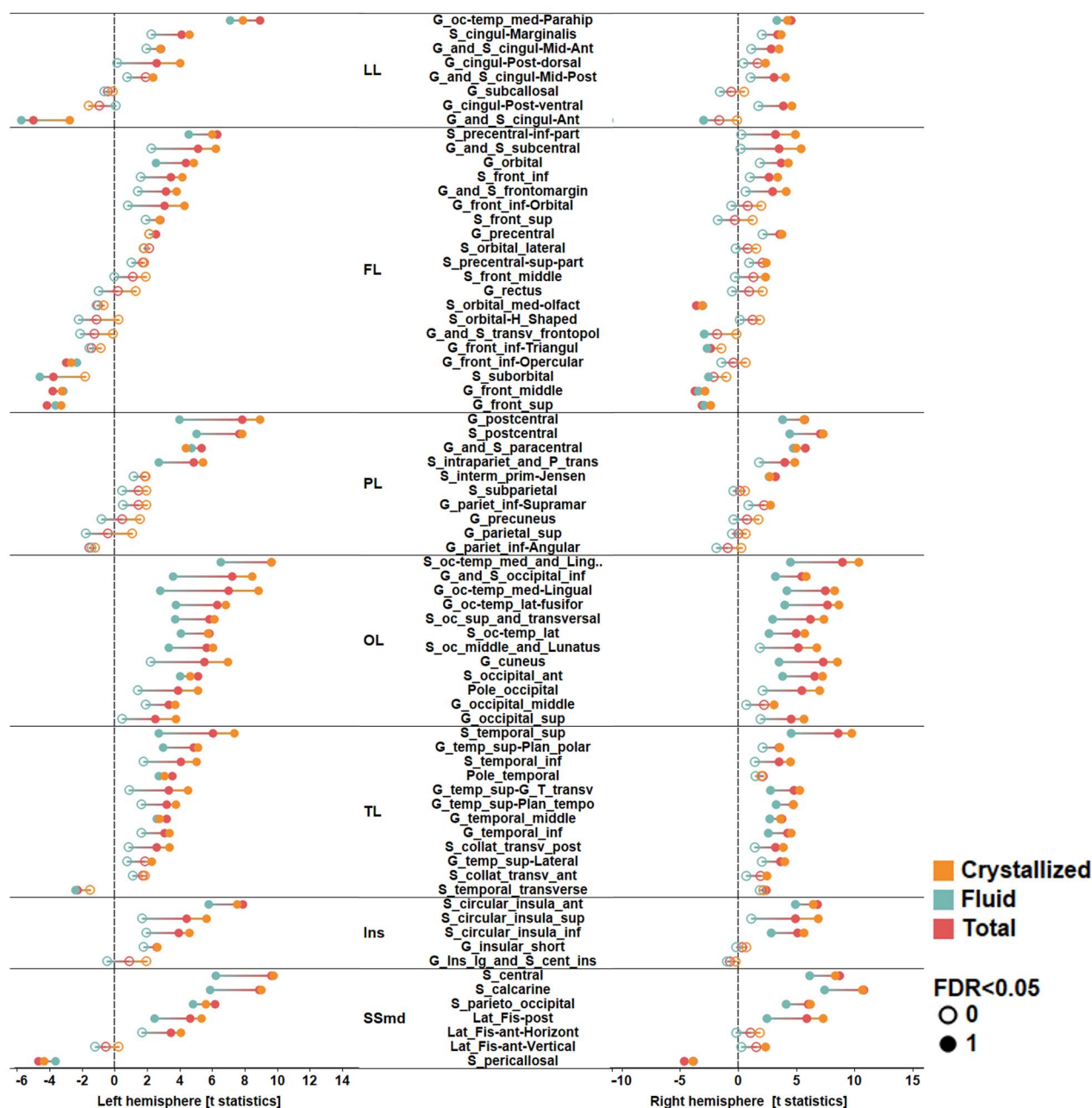
Fig. 2. The *t* value of mean model between the three kinds of intelligence (intelligence, crystallized intelligence, and fluid intelligence) indicators and region thickness of cortical regions based on the Destrieux atlas. The atlas is further broken down into limbic lobe and sulcus (LL), frontal lobe and sulcus (FL), temporal lobe and sulcus (TL), parietal lobe and sulcus (PL), occipital lobe and sulcus (OL), insular cortex (Ins), and sulci/spaces major divisions (SSmd).
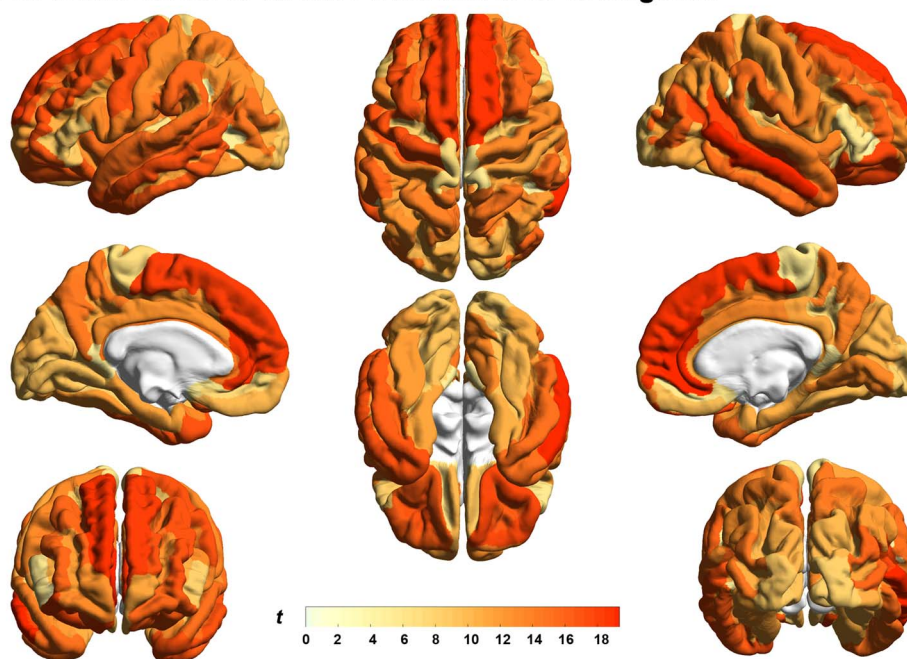
Cortical thickness dispersion across the subscales was not correlated with *g*C and *g*F subscale scores. The *g*, *g*C, and *g*F were also not associated with surface area dispersion (Supplementary Figs S5B and S6B).

Discussion

We show in this large-scale data set of >10 000 children, a critical finding that higher intelligence during a key transition point of childhood neurodevelopment (ages: 9–11 years old) is associated with dispersion or variability only in cortical thickness rather than surface area, especially in bilateral rostral cingulate and the right precuneus. We further emphasize the negative correlation across both fluid and crystallized intelligence and lower mean cortical thickness in the rostral cingulate, a finding that was robustly preserved across all subscales of measures contributing to both fluid (working and sequence memory, card sorting, flanker, and processing speed) and crystallized intelligence (vocabulary and recognition). The DGLM independently assesses the contribution of mean and dispersion, hence allowing the
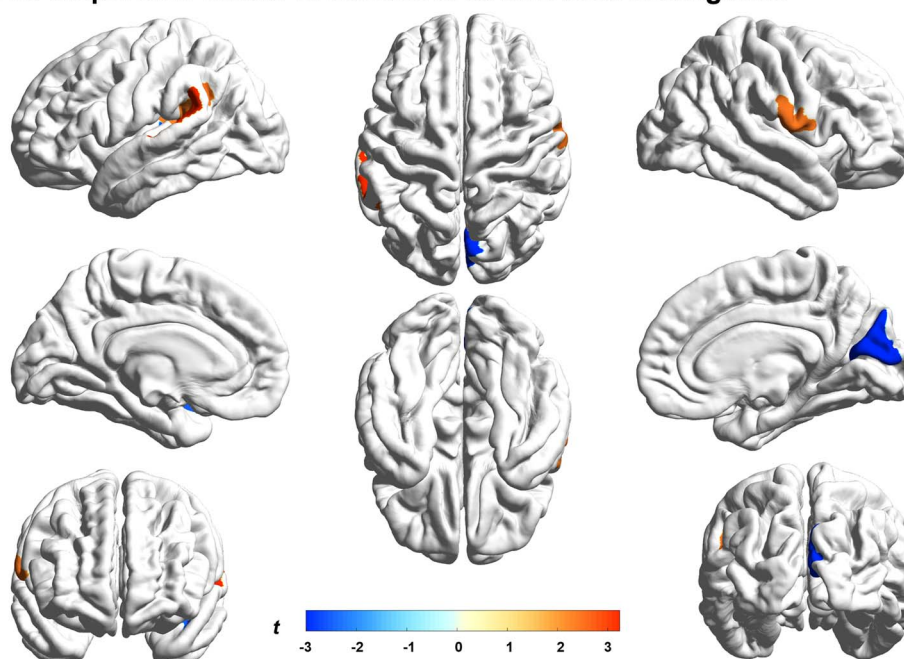
Fig. 3. Regions of interest showing surface area and dispersion significantly associated with intelligence in (A) mean and (B) dispersion model. Cortical regions of interest for which *P* value < FDR-corrected (0.05) are shown based on the Destrieux atlas.

two constructs to be dissociated. Our findings further suggest a dissociation as a function of IQ between regions implicated in executive and control processes (dorsolateral and dorsomedial prefrontal cortex) and basic processes relevant to sensory processing and goal representation and tracking in this transition neurodevelopmental age.

Mean of cortical thickness and intelligence in rostral cingulate

Previous studies show a change in the relationship between IQ and cortical thickness with age from a negative correlation in early childhood to a positive correlation in late adolescence, which is focused particularly on superior prefrontal extending into dorsomedial
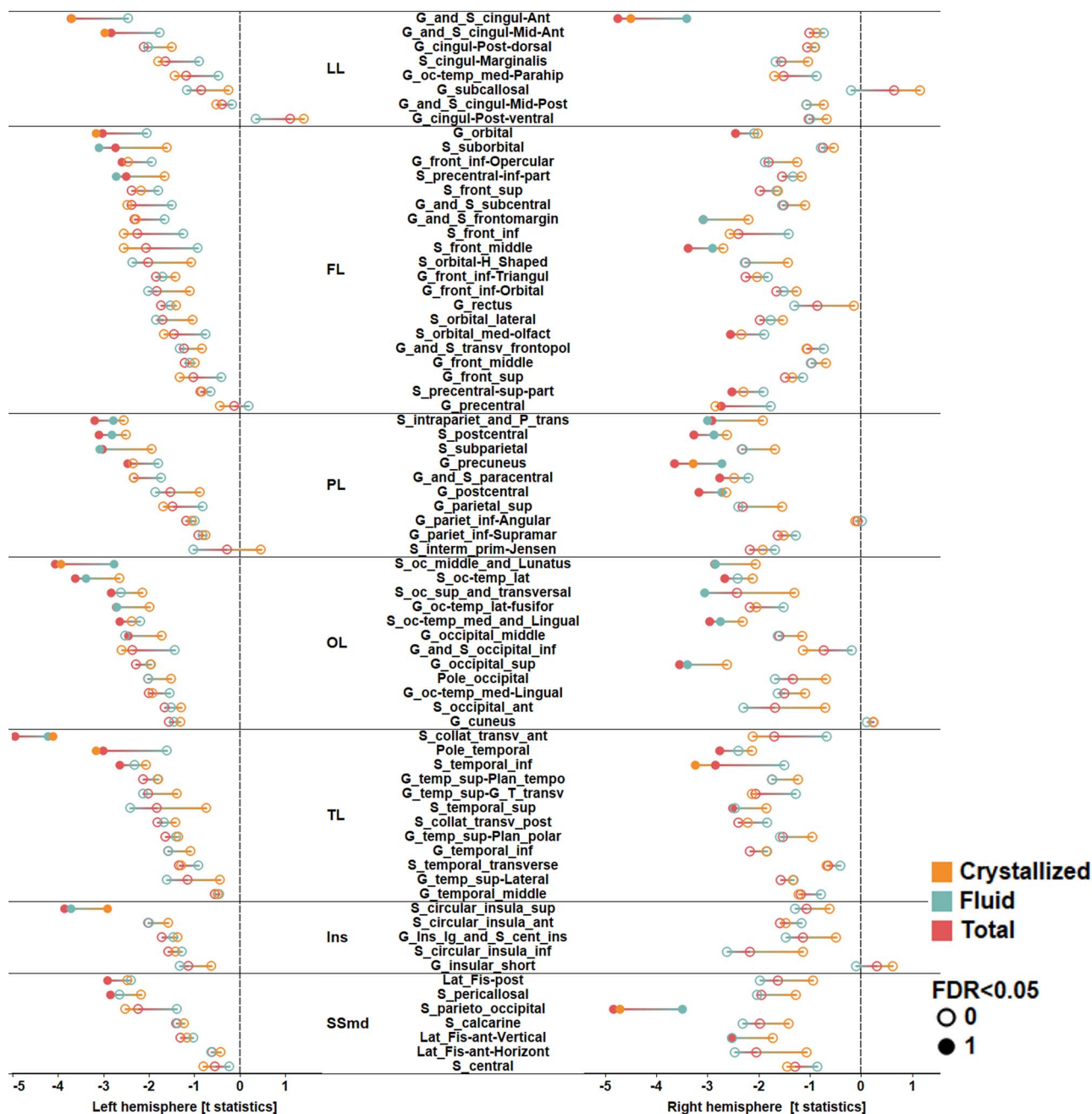
Fig. 4. The *t* value of dispersion model between the three intelligence scores and cortical thickness of ROI based on Destrieux atlas. The atlas is further broken down into limbic lobe and sulcus (LL), frontal lobe and sulcus (FL), temporal lobe and sulcus (TL), parietal lobe and sulcus (PL), occipital lobe and sulcus (OL), insular cortex (Ins), and sulci/spaces major divisions (SSmd).

prefrontal regions (Shaw et al. 2006; Goh et al. 2011). These studies examined the longitudinal trajectory across a wide age range in small samples (∼100 subjects). Here, focusing on a specific age range during which the shift from negative to positive correlation was observed, we demonstrate this same expected negative mean correlation in a much larger sample of preadolescents within the same regions consistent with early childhood, thus emphasizing the reliability of these findings. However, we emphasize that our findings extend too much wider regions than initially shown in these superior prefrontal regions. We demonstrate a critical

role for both the mean and dispersion indices of the rostral cingulate, a critical hub region that not only showed the greatest negative correlation but was also robustly shown across all intelligence subscales. The rostral cingulate is a hub region identified in tract-tracing studies across both primate and human studies (Tang et al. 2019), demonstrating convergence across prefrontal regions and suggested to play an integrative role of functions implicated in the motivational processes of valuation, choice, and action control. The rostral cingulate (BA 24 and 32) have been implicated in diverse emotional and cognitive processes (Tang et al. 2019),

including interception, action control, social cognition (theory of mind), and anxiety and fear processing and are coactivated across default mode (Greicius et al. 2003) and executive (Seeley et al. 2007) networks. Further, we also used state functional MRI in the ABCD study to verify patterns of covariation within cortical regions functionally connected in these brain networks. These results are shown in Supplementary Figure S9.

Dispersion of cortical thickness and intelligence in rostral cingulate

We further show that higher intelligence was independently associated with lower interindividual dispersion in cortical thickness in the rostral anterior cingulate and right precuneus and in orbitofrontal cortex and right somatosensory cortex. Thus, preadolescent populations with a higher IQ have a lower variation or greater structural cortical thickness similarities in these regions than those with a lower IQ. This association with cortical thickness was specific with no relationship observed with cortical surface area variation. The rostral cingulate and precuneus are also involved in state-dependent relationships with task-negative or default networks. These distributed association networks in the default network are believed to be supported by anatomical connectivity (Buckner and DiNicola 2019), thus potentially linking function and morphology in the developmental process. The precuneus is also implicated in task-positive networks and functions, such as task difficulty, retrieval of autobiographical memory, emotional processing, and monitoring reward outcomes (Utevsky et al. 2014). That the negative correlations observed with orbitofrontal and somatosensory cortex cortical thickness dispersion appear to be driven by gC and gF, respectively, suggest that these basic functions may be differentiated: Crystallized intelligence may be more closely related to flexible tracking of goals and fluid intelligence with basic sensory processes.

Dissociable relationships between cortical thickness and intelligence from mean model

We further highlight a negative correlation across the lateral and inferior prefrontal cortexes. In much older age groups, these regions are usually positively rather than negatively correlated with IQ (Hampshire et al. 2011). Studies (Choi et al. 2008; Menary et al. 2013; Karama et al. 2014; Yuan et al. 2018; Tadayon et al. 2020) demonstrate a positive relationship between cortical thickness in multiple regions and intelligence within older age groups. By contrast, we show a negative relationship with IQ, a relationship that has not been previously demonstrated, suggesting that, these regions, like that of the superior prefrontal and dorsomedial prefrontal cortexes (Squeglia LM et al. 2013; Chaddock-Heyman L et al. 2015) if followed longitudinally, may also have a similar U-shaped relationship with IQ as a function of age.

We further show a positive relationship between intelligence and the orbitofrontal cortex and also with

regions involved with basic sensory processing (primary somatosensory and secondary visual cortices) and object and face representations (mesial and inferotemporal regions). Thus, in this transitional age group, we emphasize a unique dissociation in the direction of the relationship between superior, lateral, and medial prefrontal, which show a negative correlation with IQ as contrasted with orbitofrontal cortices which show a positive correlation with IQ. These regions are involved in very different functional processes with dorsolateral regions implicated in higher-order abstract executive and action control regions as compared to orbitofrontal cortices implicated in more concrete tracking of positive and negative goals to flexibly guide behaviors (Zald and Rauch 2006; Rolls 2019a, 2019b). Thus, our findings emphasize a more nuanced relationship between cortical regions implicated in IQ than previous studies when focusing on a larger sample and a tighter transitional age range.

Contrasting cortical thickness and surface area relationships with intelligence

In contrast to the differential valence of correlation observed with mean cortical thickness, we show solely positive correlations with intelligence and mean surface area across all cortical regions. The first step in the evolutionary ascent of the human cerebral cortex has been theorized to be enlargement, which occurs mainly by the expansion of the surface area without a comparable increase in its thickness (Rakic 2009). Taken together, these results suggest that the frontal lobe surface area might enlarge first, with thickness increasing later for preadolescents with higher IQ. Cortical thickness and surface area are both highly heritable but appear to be unrelated genetically (Panizzon et al. 2009). From a neuronal perspective, cortical thickness is associated with radial neuronal migration and number of neurons, dendritic arborizations, and glial support in cortical columns, while surface area is related to tangential neuronal migration and captures mini-columnar units in the cortex (Chenn and Walsh 2003; Rakic 2009; Rakic et al. 2009; Tadayon et al. 2019). Inter-regional profiles of cortical thinning related to expression profiles for marker genes of CA1 pyramidal cells, astrocytes, and microglia during development. Greater gene expression related to less thinning in development (Vidal-Pineiro et al. 2020). In childhood and adolescence, astrocytic and microglia relate to regional preservation of cortical thickness by promoting and supporting neuronal development, such as dendritic arborization and synaptic remodeling1. Whitaker and Natu (Whitaker et al. 2016; Natu et al. 2019) suggested intracortical myelination as a primary driver of cortical thinning in the adolescent cortex. The combined measures of cortical thickness and surface area accounted for 14% of the total variance of the cognition total composite score, which was greater than each measure, respectively. Thus, cortical thickness

and surface area appear to contribute to different aspects of *g*.

Conclusion

Our findings highlight the heterogeneity of morphological neurodevelopment and its contribution to intelligence at a key neurodevelopmental juncture. We highlight a potential dissociation between the higher-order executive, self-control, and motivational prefrontal function and more basic processes of sensory processing, object and feature representation, and flexible tracking of goals in the contribution of neurodevelopment to intelligence. These findings are particularly evident in the rostral cingulate, a key region involved in the integration of motivational processes. In particular, the observation of both lower mean cortical thickness and greater interindividual similarity in the rostral cingulate highlights that its delayed development is important and suggesting potentially evolutionary conservation. Thus, prior to the complex physical, hormonal, emotional, and social changes associated with puberty and adolescence, intelligence appears to be reliant on the development of more basic cognitive processes with higher-order and motivational processes presumably becoming more important at a later age. Further longitudinal studies are indicated to assess the long-term developmental trajectory and its relationship with intelligence and longer-term functional relevance to aptitude and achievement.

Limitations

Our findings have particular strengths, including a large homogeneous data set based on harmonized analysis protocols, with robust to strict procedures for removing outliers and quality assessment. However, the study is not without limitations. An important source of heterogeneity in this case–control sample may be related to different scan sites. Investigation of such effects requires carefully controlled settings and is difficult to address in large-scale multisite studies. Another possible limitation is that the increased variability is caused by movement artifacts, which are typically greater in adolescent populations (Reuter et al. 2015). Disentangling the sources of heterogeneity in the adolescence likely requires further longitudinal investigation of life span trajectories and aberrant developmental paths (Alnaes et al. 2018).

Supplementary material

Supplementary material can be found at *Cerebral Cortex* online.

Funding

Notes

References

Akshoomoff N, Beaumont JL, Bauer PJ, Dikmen SS, Gershon RC, Mungas D, Slotkin J, Tulsky D, Weintraub S, Zelazo PD et al. 2013. VIII. NIH Toolbox Cognition Battery (CB): composite scores of crystallized, fluid, and overall cognition. *Monogr Soc Res Child Dev*. 78:119–132.

Alnaes D, Kaufmann T, Doan NT, Cordova-Palomera A, Wang Y, Bettella F, Moberget T, Andreassen OA, Westlye LT. 2018. Association of heritable cognitive ability and psychopathology with white matter properties in children and adolescents. *JAMA Psychiat*. 75:287–295.

Alnaes D, Kaufmann T, van der Meer D, Cordova-Palomera A, Rokicki J, Moberget T, Bettella F, Agartz I, Barch DM, Bertolino A et al. 2019. Brain heterogeneity in schizophrenia and its association with polygenic risk. *JAMA Psychiat*. 76:739–748.

Arain M, Haque M, Johal L, Mathur P, Nel W, Rais A, Sandhu R, Sharma S. 2013. Maturation of the adolescent brain. *Neuropsychiatr Dis Treat*. 9:449–460.

Benjamini Y, Hochberg Y. 1995. Controlling the false discovery rate: a practical and powerful approach to multiple testing. *J R Stat Soc B Methodol*. 57:289–300.

Brans RG, Kahn RS, Schnack HG, van Baal GC, Posthuma D, van Haren NE, Lepage C, Lerch JP, Collins DL, Evans AC et al. 2010. Brain plasticity and intellectual ability are influenced by shared genes. *J Neurosci*. 30:5519–5524.

Brown TT, Jernigan TL. 2012. Brain development during the preschool years. *Neuropsychol Rev*. 22:313–333.

Buckner RL, DiNicola LM. 2019. The brain's default network: updated anatomy, physiology and evolving insights. *Nat Rev Neurosci*. 20:593–608.

Casey BJ, Cannonier T, Conley MI, Cohen AO, Barch DM, Heitzeg MM, Soules ME, Teslovich T, Dellarco DV, Garavan H et al. 2018. The Adolescent Brain Cognitive Development (ABCD) study: imaging acquisition across 21 sites. *Dev Cogn Neurosci*. 32:43–54.

Chenn A, Walsh CA. 2003. Increased neuronal production, enlarged forebrains and cytoarchitectural distortions in beta-catenin over-expressing transgenic mice. *Cereb Cortex*. 13:599–606.

Choi YY, Shamosh NA, Cho SH, DeYoung CG, Lee MJ, Lee JM, Kim SI, Cho ZH, Kim K, Gray JR et al. 2008. Multiple bases of human intelligence revealed by cortical thickness and neural activation. *J Neurosci*. 28:10323–10329.

Chaddock-Heyman L, Erickson KI, Kienzler C, King M, Pontifex MB, Raine LB, Hillman CH, Kramer AF. 2015. The role of aerobic fitness in cortical thickness and mathematics achievement in preadolescent children. *PloS one*. 10:e0134115.

Deary IJ, Caryl PG. 1997. Neuroscience and human intelligence differences. *Trends Neurosci*. 20:365–371.

Destrieux C, Fischl B, Dale A, Halgren E. 2010. Automatic parcellation of human cortical gyri and sulci using standard anatomical nomenclature. *Neuroimage*. 53:1–15.

Diederich A. 2007. Generalized additive models. An introduction with R. *J Math Psychol*. 51:339–339.

Dunn PK, Smyth GK. 2012. *dglm: double generalized linear models*. R package version. 1.6.2. URL: http://CRAN.R-project.org/package=dglm.

Efron B. 1986. Double exponential families and their use in generalized linear regression. *J Am Stat Assoc*. 81:709–721.

Emery NJ, Clayton NS. 2005. Evolution of the avian brain and intelligence. *Curr Biol*. 15:R946–R950.

Fuhrmann D, Knoll LJ, Blakemore SJ. 2015. Adolescence as a sensitive period of brain development. *Trends Cogn Sci*. 19:558–566.

Genc E, Fraenz C, Schluter C, Friedrich P, Hossiep R, Voelkle MC, Ling JM, Gunturkun O, Jung RE. 2018. Diffusion markers of dendritic density and arborization in gray matter predict differences in intelligence. *Nat Commun*. 9:1905.

Gilbert SL, Dobyns WB, Lahn BT. 2005. Genetic links between brain development and brain evolution. *Nat Rev Genet*. 6:581–590.

Goh S, Bansal R, Xu D, Hao X, Liu J, Peterson BS. 2011. Neuroanatomical correlates of intellectual ability across the life span. *Dev Cogn Neurosci*. 1:305–312.

Greicius MD, Krasnow B, Reiss AL, Menon V. 2003. Functional connectivity in the resting brain: a network analysis of the default mode hypothesis. *Proc Natl Acad Sci U S A*. 100:253–258.

Gu J, Kanai R. 2014. What contributes to individual differences in brain structure? *Front Hum Neurosci*. 8:262.

Hagler DJ, Hatton S, Cornejo MD, Makowski C, Fair DA, Dick AS, Sutherland MT, Casey BJ, Barch DM, Harms MP et al. 2019. Image processing and analysis methods for the Adolescent Brain Cognitive Development Study. *Neuroimage*. 202:116091.

Hampshire A, Thompson R, Duncan J, Owen AM. 2011. Lateral prefrontal cortex subregions make dissociable contributions during fluid reasoning. *Cereb Cortex*. 21:1–10.

Heaton RK, Akshoomoff N, Tulsky D, Mungas D, Weintraub S, Dikmen S, Beaumont J, Casaletto KB, Conway K, Slotkin J et al. 2014. Reliability and validity of composite scores from the NIH Toolbox Cognition Battery in adults. *J Int Neuropsychol Soc*. 20:588–598.

Karama S, Bastin ME, Murray C, Royle NA, Penke L, Munoz Maniega S, Gow AJ, Corley J, Hernandez MV, Lewis JD et al. 2014. Childhood cognitive ability accounts for associations between cognitive ability and brain cortical thickness in old age. *Mol Psychiatry*. 19:555–559.

Karama S, Colom R, Johnson W, Deary IJ, Haier R, Waber DP, Lepage C, Ganjavi H, Jung R, Evans AC et al. 2011. Cortical thickness correlates of specific cognitive performance accounted for by the general factor of intelligence in healthy children aged 6 to 18. *Neuroimage*. 55:1443–1453.

Luciana M, Bjork JM, Nagel BJ, Barch DM, Gonzalez R, Nixon SJ, Banich MT. 2018. Adolescent neurocognitive development and impacts of substance use: overview of the Adolescent Brain Cognitive Development (ABCD) baseline neurocognition battery. *Dev Cogn Neurosci*. 32:67–79.

Menary K, Collins PF, Porter JN, Muetzel R, Olson EA, Kumar V, Steinbach M, Lim KO, Luciana M. 2013. Associations between cortical thickness and general intelligence in children, adolescents and young adults. *Intelligence*. 41:597–606.

Narr KL, Woods RP, Thompson PM, Szeszko P, Robinson D, Dimtcheva T, Gurbani M, Toga AW, Bilder RM. 2007. Relationships between IQ and regional cortical gray matter thickness in healthy adults. *Cereb Cortex*. 17:2163–2171.

Natu VS, Gomez J, Barnett M, Jeska B, Kirilina E, Jaeger C, Zhen Z, Cox S, Weiner KS, Weiskopf N. 2019. Apparent thinning of human visual cortex during childhood is associated with myelination. *Proc Natl Acad Sci*. 116:20750–20759.

Ostby Y, Tamnes CK, Fjell AM, Westlye LT, Due-Tonnessen P, Walhovd KB. 2009. Heterogeneity in subcortical brain development: a structural magnetic resonance imaging study of brain maturation from 8 to 30 years. *J Neurosci*. 29:11772–11782.

Panizzon MS, Fennema-Notestine C, Eyler LT, Jernigan TL, Prom-Wormley E, Neale M, Jacobson K, Lyons MJ, Grant MD, Franz CE et al. 2009. Distinct genetic influences on cortical surface area and cortical thickness. *Cereb Cortex*. 19:2728–2735.

Paula GA. 2013. On diagnostics in double generalized linear models. *Comput Stat Data Anal*. 68:44–51.

Pietschnig J, Penke L, Wicherts JM, Zeiler M, Voracek M. 2015. Meta-analysis of associations between human brain volume and intelligence differences: How strong are they and what do they mean? *Neurosci Biobehav Rev*. 57:411–432.

Posthuma D, De Geus EJC, Baare WFC, Pol HEH, Kahn RS, Boomsma DI. 2002. The association between brain volume and intelligence is of genetic origin. *Nat Neurosci*. 5:83–84.

Rakic P. 2009. Evolution of the neocortex: a perspective from developmental biology. *Nat Rev Neurosci*. 10:724–735.

Rakic P, Ayoub AE, Breunig JJ, Dominguez MH. 2009. Decision by division: making cortical maps. *Trends Neurosci*. 32:291–301.

Reuter M, Tisdall MD, Qureshi A, Buckner RL, van der Kouwe AJW, Fischl B. 2015. Head motion during MRI acquisition reduces gray matter volume and thickness estimates. *Neuroimage*. 107:107–115.

Rolls ET. 2019a. *The orbitofrontal cortex*. Oxford, United Kingdom: Oxford University Press.

Rolls ET. 2019b. The orbitofrontal cortex and emotion in health and disease, including depression. *Neuropsychologia*. 128:14–43.

Seeley WW, Menon V, Schatzberg AF, Keller J, Glover GH, Kenna H, Reiss AL, Greicius MD. 2007. Dissociable intrinsic connectivity networks for salience processing and executive control. *J Neurosci*. 27:2349–2356.

Shaw P, Greenstein D, Lerch J, Clasen L, Lenroot R, Gogtay N, Evans A, Rapoport J, Giedd J. 2006. Intellectual ability and cortical development in children and adolescents. *Nature*. 440:676–679.

Smyth GK. 1989. Generalized linear models with varying dispersion. *J R Stat Soc B Methodol*. 51:47–60.

Smyth GK, Verbyla AP. 1999. Adjusted likelihood methods for modelling dispersion in generalized linear models. *Environ*. 10:695–709.

Sowell ER, Thompson PM, Leonard CM, Welcome SE, Kan E, Toga AW. 2004. Longitudinal mapping of cortical thickness and brain growth in normal children. *J Neurosci*. 24:8223–8231.

Squeglia LM, Jacobus J, Sorg SF, Jernigan TL, Tapert SF. 2013. Early adolescent cortical thinning is related to better neuropsychological performance. *J Int Neuropsychol Soc*. 19:962–970.

Tadayon E, Pascual-Leone A, Santarnecchi E. 2019. Differential contribution of cortical thickness, surface area, and gyrification to fluid and crystallized intelligence. *Cereb Cortex*. 30:215–225.

Tadayon E, Pascual-Leone A, Santarnecchi E. 2020. Differential contribution of cortical thickness, surface area, and gyrification to fluid and crystallized intelligence. *Cereb Cortex*. 30:215–225.

Tang W, Jbabdi S, Zhu Z, Cottaar M, Grisot G, Lehman JF, Yendiki A, Haber SN. 2019. A connectional hub in the rostral anterior cingulate cortex links areas of emotion and cognitive control. *Elife*. 8:e43761.

Unsworth N, Fukuda K, Awh E, Vogel EK. 2014. Working memory and fluid intelligence: capacity, attention control, and secondary memory retrieval. *Cogn Psychol*. 71:1–26.

Utevsky AV, Smith DV, Huettel SA. 2014. Precuneus is a functional core of the default-mode network. *J Neurosci*. 34:932–940.

Vidal-Pineiro D, Parker N, Shin J, French L, Grydeland H, Jackowski AP, Mowinckel AM, Patel Y, Pausova Z, Salum G et al. 2020. Cellular correlates of cortical thinning throughout the lifespan. *Sci Rep*. 10:21803.

Whitaker KJ, Vértes PE, Romero-Garcia R, Váša F, Moutoussis M, Prabhu G, Weiskopf N, Callaghan MF, Wagstyl K, Rittman T. 2016. Adolescence is associated with genomically patterned consolidation of the hubs of the human brain connectome. *Proc Natl Acad Sci*. 113:9105–9110.

Wood S. 2017. mgcv: Mixed GAM Computation Vehicle with Automatic Smoothness Estimation (Version 1.8-22). In.

Yuan P, Voelkle MC, Raz N. 2018. Fluid intelligence and gross structural properties of the cerebral cortex in middle-aged and older adults: a multi-occasion longitudinal study. *Neuroimage*. 172: 21–30.

Zald DH, Rauch SL. 2006. *The orbitofrontal cortex*. Oxford, New York: Oxford University Press.

Zaval L, Li Y, Johnson EJ, Weber EU. 2015. Complementary contributions of fluid and crystallized intelligence to decision making across the life span. In: *Aging and decision making*. Academic Press: Elsevier, pp. 149–168.